Journal of Catalysis **187,** 332–342 (1999)
Article ID jcat.1999.2618, available online at http://www.idealibrary.com on IDEAL®

Microcalorimetry, Adsorption, and Reaction Studies of CO, O_2, and $CO + O_2$ over Au/Fe_2O_3, Fe_2O_3, and Polycrystalline Gold Catalysts

A. K. Tripathi, V. S. Kamble, and N. M. Gupta[1]

Applied Chemistry Division, Bhabha Atomic Research Centre, Trombay, Mumbai 400 085, India

Received February 10, 1999; revised May 18, 1999; accepted June 30, 1999

To understand the effect of catalytic activity of Au/Fe_2O_3 at low temperatures on a CO oxidation reaction, adsorption and changes in enthalpy were determined for the interaction of CO, O_2, or $CO + O_2$ (2 : 1) pulses over Au (5 at.%)/Fe_2O_3, Fe_2O_3, and polycrystalline gold catalysts between 300 and 470 K. The results demonstrate that the oxidation of CO on both Fe_2O_3 and Au/Fe_2O_3 occur by means of similar redox mechanisms involving the removal and replenishment of lattice oxygen, where the presence of gold promotes these processes. The FTIR data reveal that gold facilitates the chemisorption of CO on Au/Fe_2O_3, leading predominantly to the formation of Au^0–CO species. The carbonate-like species, formed on both Fe_2O_3 and Au/Fe_2O_3 during the adsorption of CO or $CO + O_2$, are stable below 375 K and are regarded to be mere by-products that do not play a major role in the CO oxidation process, particularly at low reaction temperatures (<400 K). The larger gold particles inhibited the formation of CO_{ad} species during exposure of Au/Fe_2O_3 to $CO + O_2$; this was accompanied by a decrease in the adsorption of both CO and O_2 and a decrease in the formation of CO_2. The promotional effect of gold is attributed to the presence of small (nanosize) Au crystallites that facilitate the chemisorption of CO molecules because of their inherent defective structural sites. It is suggested that the energy that evolves during the chemisorption of CO molecules is responsible for the surge in temperature at the Au–Fe_2O_3 interfaces; these eventually serve as sites for the accelerated reaction between CO and the support. © 1999 Academic Press

Key Words: **adsorption and oxidation of CO; microcalorimetry study; FTIR study; mechanism of; gold catalyst; particle size effect in; role of gold in.**

INTRODUCTION

Gold is regarded to be a catalytically inactive metal because of its $5d^{10}$ configuration. Recent publications have, however, revealed that gold has a high catalytic activity when it is dispersed over reducible metal oxides, particularly in the oxidation of CO at low temperatures (1–7). The preparation conditions and the size of the gold particles are important for the high activity of supported gold catalysts, as emphasized in numerous studies (1, 8). Haruta *et al.* (1, 2) reported that the small gold particles not only act as the sites for the reversible adsorption of CO, but they also favor the adsorption of oxygen on the oxide support. They proposed a mechanism involving the migration of CO to the metal support interface and the formation of bidentate carbonate species, where the decomposition of the carbonate-like species is considered to be the rate-determining step (7). Recent studies, on one hand, propose that Au^{1+} species are more active toward the oxidation of CO compared to the Au^0 sites (9–11). Boccuzzi *et al.* (12), on the other hand, proposed two independent pathways for CO oxidation on Au/ZnO and Au/TiO_2 catalysts, one leading to the direct oxidation of CO at the surface of the metallic particles and the other to a slowly induced oxidation of CO involving the lattice oxygen of the support. The individual roles of gold and the oxide support and the reaction routes responsible for the catalytic activity of supported gold are not fully understood.

In previous publications (13–15), we used microcalorimetry to gain insight into surface processes occurring during the adsorption and oxidation of CO over supported noble metal catalysts. These studies emphasized the importance of the chemical nature of the catalyst surface during the CO/O_2 interaction and of the energy released during the chemisorption of the reacting gases at the metal/support interfaces. Using similar methods in the present study, we used a heat-flow microcalorimeter to measure changes in the enthalpy during exposure of the Au/Fe_2O_3 catalyst to CO, O_2, and $CO + O_2$ (2 : 1) pulses at different temperatures (300–470 K). The effect of surface coverage was evaluated by dosing successive pulses of these adsorbates. The fraction of these gases adsorbed over the catalyst surface and the reaction products formed at different stages were analyzed simultaneously using a gas chromatograph attached to the sample cell. To compare the results, parallel experiments were performed using metal-free Fe_2O_3 and polycrystalline gold samples. The effect of calcination of a catalyst at temperatures ranging from 670 to 970 K on the

[1] To whom correspondence should be addressed. Fax: 091-22-5505151. E-mail: nmgupta@magnum.barc.ernet.in.

0021-9517/99 $30.00

thermochemical data and on the reaction products formed was evaluated to understand the role of the particle size of gold in the adsorption and catalytic activity of Au/Fe_2O_3.

EXPERIMENTAL

Catalyst

The Au/Fe_2O_3 catalyst was prepared according to a method reported previously (1, 16). A gold-free Fe_2O_3 sample was prepared using a similar procedure. The samples were calcined at 673 K (4 h) before use. The polycrystalline gold powder sample was prepared by the chemical reduction of $HAuCl_4$ using a formaldehyde solution. The black precipitate thus obtained was dried and then heated in O_2 at 673 K for about 4 h to obtain pure gold powder.

The N_2 BET surface area of the Au/Fe_2O_3 and Fe_2O_3 samples was found to be 45 and 41 $m^2\ g^{-1}$ respectively, but measuring the metal surface area of Au/Fe_2O_3 according to an O_2 chemisorption method did not give reliable results. The XRD pattern of these samples matched that of α-Fe_2O_3 (hematite). The gold content in Au/Fe_2O_3, as determined by the atomic absorption method, was about 5 at.%. TEM micrographs were recorded with a Jeol microscope (model-2000 FX) using the standard technique of grinding and deposition over a copper grid.

Microcalorimetry

The differential heat (q_d) evolved during interaction of an adsorbate pulse over a catalyst surface was evaluated using a heat-flow microcalorimeter (C-80, Setaram, France), equipped with a set of stainless steel gas circulation cells. Our previous publications give the details of this procedure (13, 14). A 200-mg sample ($\sim$150-μm particle size) was placed in the sample vessel, while the reference vessel was empty. The stainless steel plumbing system attached to the equipment enabled the evacuation of both vessels ($\sim 10^{-3}$ Torr) or, alternatively, permitted an identical flow of gas through them. A number of adsorbate pulses (4.1-μmol each) were dosed successively into the sample cell about every 15 min, and the effluents were analyzed using a set of thermal conductivity detectors, one connected to a Porapak-T (0.5 m, 3-mm i.d.) column and the other to a molecular sieve-5A (0.3 m, 3-mm i.d.) column. The GC system was kept at room temperature.

Before the adsorbate pulse was injected, the catalyst sample was pretreated *in situ* at 473 K for 1 h in a flow of O_2 (20 ml min^{-1}) followed by evacuation (1 h) and heating for 1 h at the same temperature in a flow of He (20 ml min^{-1}). The catalyst was then kept in a flow of He at the experimental temperature. The calorimeter response was calibrated using a standard joule calibrator. Au/Fe_2O_3 samples, calcined at different temperatures from 650 to 1000 K, were also used for microcalorimetry to evaluate the effect of the particle size of the gold.

Infrared Spectroscopy

The high-pressure high-vacuum IR cell used in this study was described earlier (17). A 25-mm diameter self-supporting sample wafer (18 mg/cm^2) was heated *in situ* for 2 h in a flow of O_2 at 473 K followed by evacuation at 523 K. The background spectrum was recorded after the sample was cooled to the required temperature and before it was exposed to a dose of 100 Torr CO or $CO + O_2$ (2 : 1). The difference spectra were obtained by subtracting the spectrum of gaseous CO from the spectrum recorded after exposure of the sample to the adsorbate. For each spectrum, 300 scans were recorded in transmittance mode at a resolution of 4 cm^{-1} using a Mattson (USA) Cygnus-100 FTIR equipped with a DTGS detector.

Catalyst Activity

The activity of the catalysts was evaluated for the CO oxidation reaction in the temperature range of 273–673 K using a flow-through quartz microreactor 8 mm in diameter. For this purpose, 500 mg of a 40- to 80-mesh fraction of a powdered catalyst sample was packed between two quartz wool plugs; a gas mixture of $CO + O_2 + He$ (2 : 1 : 17) was passed through the microreactor at a flow rate of 1200 ml $h^{-1}\ g^{-1}$. The product analysis was carried out using a GC equipped with a thermal conductivity detector and a Porapak-Q column, both at room temperature. Carbon monoxide (Airco, USA) and oxygen (Indian Oxygen, Iolar grade) were used after purification (17).

RESULTS

Characterization

About 75% of the gold particles in Au/Fe_2O_3 were 3–5 nm in size, while the average particle size was around 4.8 nm, as revealed by TEM measurements. The size of the gold crystallite increased when Au/Fe_2O_3 was calcined in air or oxygen at temperatures above 700 K. Thus, calcination of a sample at 873 K gave rise to gold particles, 5–20 nm in size with the average particle size being $\sim$11 nm. Figures 1a and 1b show the typical particle size distribution of gold in Au/Fe_2O_3 samples calcined at 673 and 873 K, respectively. We measured about 100 particles on TEM micrographs.

XPS measurements on Au/Fe_2O_3, made using a Riber XPS system (model CX-700) consisting of a Mg/Al twin anode X-ray source, gave gold signals at binding energies of 83.87 eV ($4f_{7/2}$) and 87.4 eV ($4f_{5/2}$), corresponding to the Au^0 state of gold metal. An XPS band, due to the higher oxidation state of gold, was not detected.

CO Adsorption

Au/Fe_2O_3 sample. When several pulses of carbon monoxide were introduced at a particular temperature at

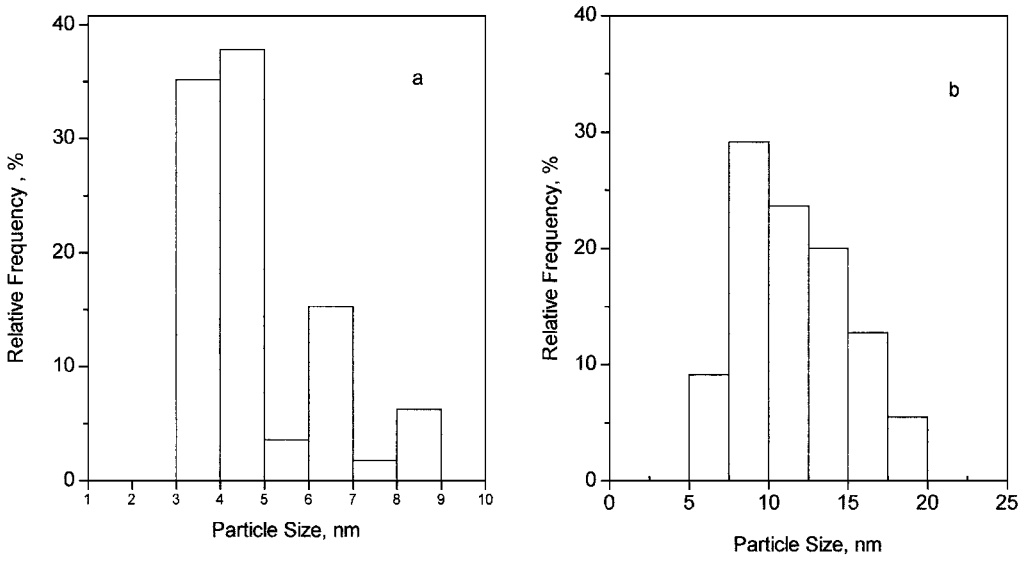

FIG. 1. Distribution of gold according to particle size in an Au/Fe_2O_3 catalyst calcined at (a) 670 K and (b) 870 K.

intervals of ~15 min, the amount of CO adsorbed decreased only slightly for successive pulses. Some of the adsorbed CO was oxidized to CO_2, and the extent of CO adsorption and conversion of adsorbed CO to CO_2 depended on the catalyst temperature. Thus, the average fraction of CO, adsorbed/reacted from 5 to 6 pulses, increases from about 40 to 65% with increasing sample temperature (300–470 K) (Fig. 2a). Similarly, $CO_{ad} \rightarrow CO_2$ conversion, on one hand increased from 2 to 60% as the temperature of the sample rose (Fig. 2b). On the other hand, a similar amount of heat (110–120 kJ mol^{-1}) was produced during CO exposure at different temperatures (Fig. 2c).

Fe_2O_3 sample. Compared to the data in Fig. 2a, only a very small fraction of CO was adsorbed/reacted when a Fe_2O_3 sample was exposed to carbon monoxide pulses at temperatures below 400 K; no CO_2 was formed. However, the fraction of CO adsorbed and the yield of CO_2 increased considerably at higher temperatures. Thus, about 48% of CO was adsorbed at 470 K compared to ~7% at 370 K (Fig. 3a). Similarly, about 45% of CO_{ad} converted to CO_2

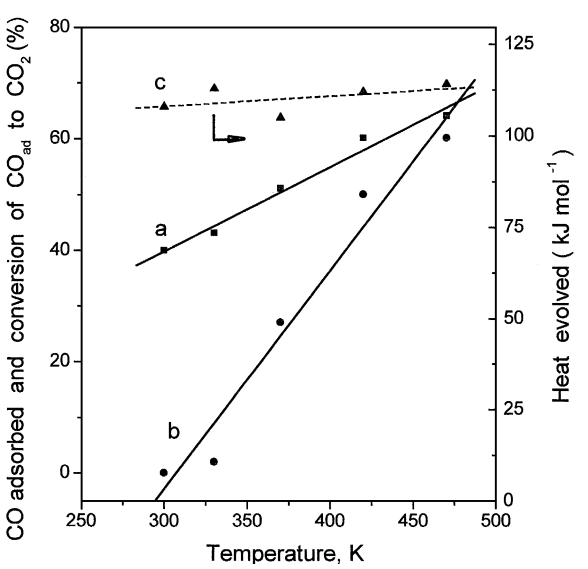

FIG. 2. Average amount of CO adsorbed/reacted (a) and conversion of CO_{ad} to CO_2 (b) when an Au/Fe_2O_3 catalyst was exposed to five pulses of 4.1 μmol of CO at different temperatures. Curve c shows the differential heat evolved in the process.

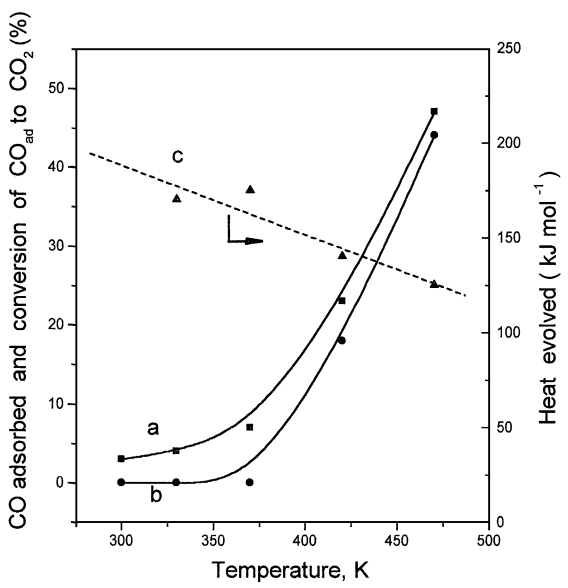

FIG. 3. Average amount of CO adsorbed/reacted (a) and conversion of CO_{ad} to CO_2 (b) when a Fe_2O_3 catalyst was exposed to five pulses of 4.1 μmol of CO at different temperatures. Curve c shows the amount of heat evolved in the process.

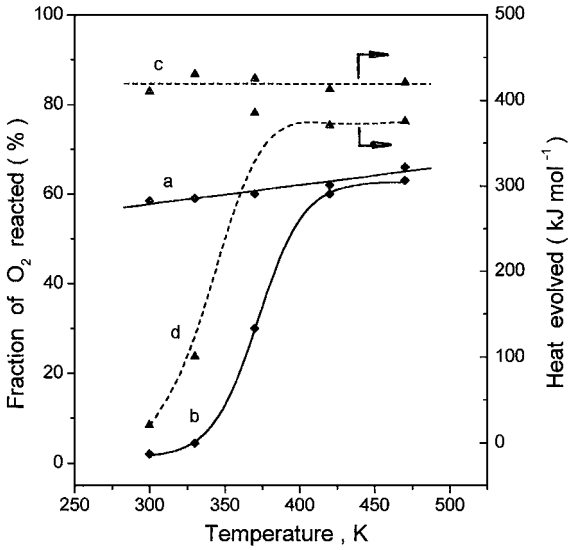

FIG. 4. Fraction of O_2 reacted and the differential heat evolved when Au/Fe_2O_3 and Fe_2O_3 catalysts were exposed to a pulse of 4.1 μmol of O_2 following exposure to 10 pulses of CO and flushing in He at different temperatures. (a, c) Au/Fe_2O_3; (b, d) Fe_2O_3.

at 470 K, while no CO_2 was formed at 370 K (Fig. 3b). Compared to the heat produced with Au/Fe_2O_3 (Fig. 2c), more heat ($\sim$175 kJ mol^{-1}) was produced at 300–375 K, while the q_d value at higher temperatures decreased to 130 $\pm$ 5 kJ mol^{-1} (Fig. 3c).

Gold sample. A negligible amount (3–5%) of CO was adsorbed from a pulse on a polycrystalline gold sample at 300–470 K. Except for exposure at 470 K, no CO_2 was detected. Correspondingly, the value of q_d was very small ($\sim$20–50 kJ mol^{-1}).

Interaction of O_2

Figure 4 shows the comparative data for Au/Fe_2O_3 and Fe_2O_3 samples of the fraction of adsorbed O_2 and the amount of heat that evolved as a function of temperature when the samples, that were exposed to 10 pulses of CO, were flushed with He for about 1 h and then exposed to a pulse of 4.1 μmol of O_2. Thus, at all reaction temperatures, about 60% of O_2, on one hand, was adsorbed from an O_2 pulse by the Au/Fe_2O_3 sample (Fig. 4a). On the other hand, the fraction of adsorbed/reacted O_2 in the Fe_2O_3 sample depended mainly on the reaction temperature. Thus, only about 2–5% of O_2 from a pulse was adsorbed by CO-treated Fe_2O_3 below 400 K, while considerably more O_2 was adsorbed at higher temperatures (Fig. 4b). About 425 kJ mol^{-1} of heat was produced during the first O_2 pulse over the Au/Fe_2O_3 sample that had been exposed to CO pulses (Fig. 4c). In the case of Fe_2O_3, a very small amount of heat evolved below 350 K, while at higher reaction temperatures, q_d was $\sim$370 kJ mol^{-1} (Fig. 4d). No CO_2 was detected for the O_2 pulse over Au/Fe_2O_3 and Fe_2O_3 samples, kept below 400 K after CO exposure. At higher sample temperatures, a very small amount of CO_2 ($\sim$5–7% of total CO adsorbed by a sample from 10 successive pulses) formed during subsequent interaction with O_2.

The amount adsorbed and also the q value decreased sharply after two to three successive pulses of O_2 were admitted over the Au/Fe_2O_3 or Fe_2O_3 sample, subsequent to exposure of CO as mentioned above.

In the case of the gold sample exposed to CO at different temperatures, subsequent O_2 pulse injections through a He carrier gas resulted in a negligible amount of O_2 adsorption ($\sim$2–3%), and a correspondingly small amount of heat was produced.

Adsorption of $CO + O_2$

Au/Fe_2O_3 catalyst. Figure 5 shows the average fraction of CO (curve a) and O_2 (curve b) adsorbed from a 4.1-μmol $CO + O_2$ (2 : 1) pulse injected over an Au/Fe_2O_3 catalyst at different temperatures. As seen in Fig. 5a, about 60% of CO was adsorbed/reacted from a pulse at all temperatures. The amount of O_2 adsorbed was slightly lower and varied from 50 to 60% for a rise in temperature from 300 to 470 K (Fig. 5b). CO_2 formation was detected at all temperatures, increasing from about 2% at 300 K to 70% at 470 K (Fig. 5c). Figure 5d gives the amount of heat evolved in these experiments, the q_d value varying from 175 to 210 kJ mol^{-1}, depending on the catalyst temperature.

Whereas the fraction of reacted CO or O_2 remained more or less constant for the successive pulses of $CO + O_2$ dosed

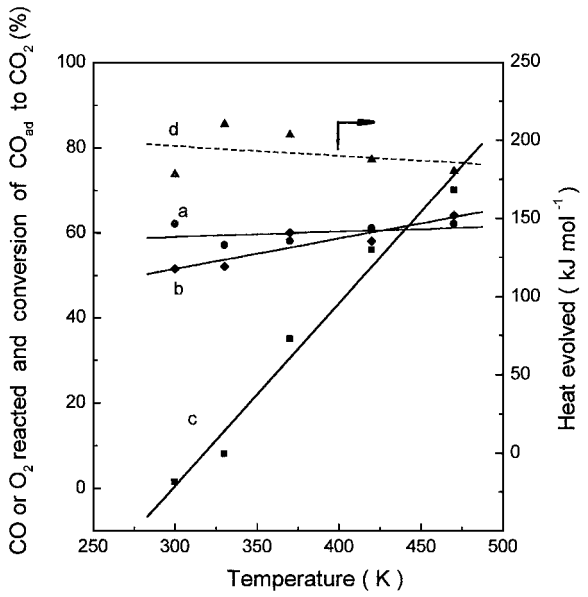

FIG. 5. Average fraction of CO (a) and O_2 (b) adsorbed/reacted and conversion of CO_{ad} to CO_2 (c) when an Au/Fe_2O_3 catalyst was exposed to five successive pulses of 4.1 μmol of $CO + O_2$ (2 : 1). Curve d shows the differential heat evolved in the process.

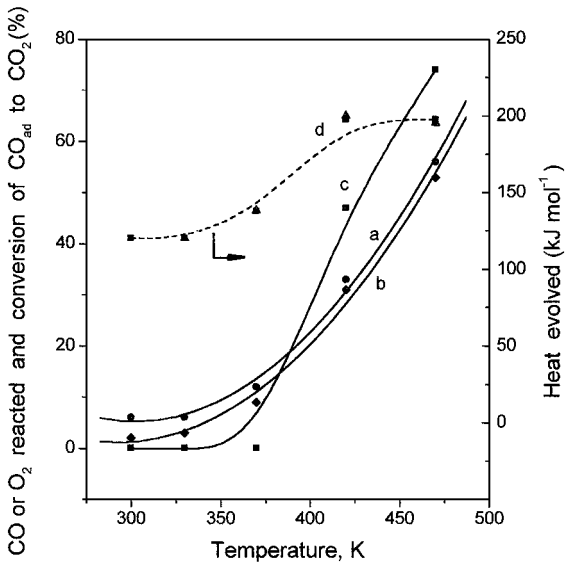

FIG. 6. Average fraction of CO (a) and O_2 (b) adsorbed/reacted and the yield of CO_2 (c) during the five dosed pulses of 4.1 μmol of $CO + O_2$ (2 : 1) on a Fe_2O_3 catalyst at different temperatures. Curve d shows the differential heat evolved in the process.

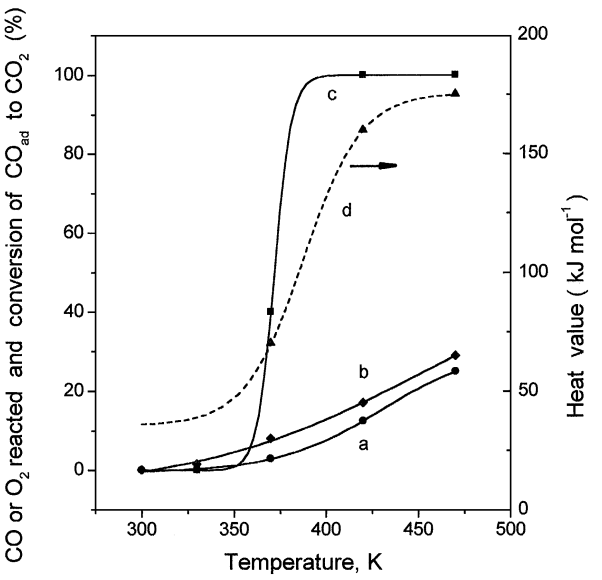

FIG. 7. Average fraction of CO (a) and O_2 (b) adsorbed/reacted and the yield of CO_2 (c) when a polycrystalline gold sample was exposed to five pulses of 4.1 μmol of $CO + O_2$ (2 : 1) at different temperatures. Curve d shows the differential heat evolved in the process.

over Au/Fe_2O_3 at different temperatures, $CO_{ad} \rightarrow CO_2$ conversion increased slightly with the second and third pulses and then reached saturation.

Fe_2O_3 catalyst. Whereas only small amounts of CO or O_2 were adsorbed/reacted and correspondingly low yields of CO_2 were observed below 400 K for interaction of $CO + O_2$ pulses over the Fe_2O_3 catalyst, the adsorption of both reactants and $CO_{ad} \rightarrow CO_2$ conversion increased considerably with a rise in temperature. Figure 6 gives the average data in curves a–c. The q value increased progressively from 120 to 200 kJ mol^{-1} with increasing temperature (Fig. 6d).

Au catalyst. Figure 7 shows the effect of the reaction temperature on the average amounts of CO and O_2 adsorbed/reacted from five $CO + O_2$ (2 : 1) pulses injected over a polycrystalline gold sample. These data show that about the same fractions of CO and O_2 were adsorbed, increasing steadily from around 2 to 30% for an increase in temperature from 330 to 470 K (curves a and b). Adsorption of CO or O_2 was not detected at room temperature. Similarly, a negligible amount of CO_2 formed at temperatures below 370 K, while $CO_{ad} \rightarrow CO_2$ conversion ranged from 40 to 100% at higher catalyst temperatures (Fig. 7c). The q_d value increased from 75 to 175 kJ mol^{-1} with an increase in temperature from 370 to 470 K (Fig. 7d).

Effect of Calcination

Figures 8 and 9 show the effect of calcination of an Au/Fe_2O_3 catalyst on CO and O_2 adsorption when pulses of $CO + O_2$ (2 : 1) were dosed at different temperatures. Adsorption of both CO and O_2 decreased considerably with increasing calcination temperature and the effect was more pronounced at lower reaction temperatures (Figs. 8 and 9 (curve a)). Even though the adsorbed fractions of CO and O_2 decreased with an increasing calcination temperature, the conversion of CO_{ad} to CO_2 increased (Fig. 10). Thus, about 45% of adsorbed CO converted to CO_2 at 370 K for the Au/Fe_2O_3 sample calcined at 670 K, whereas the

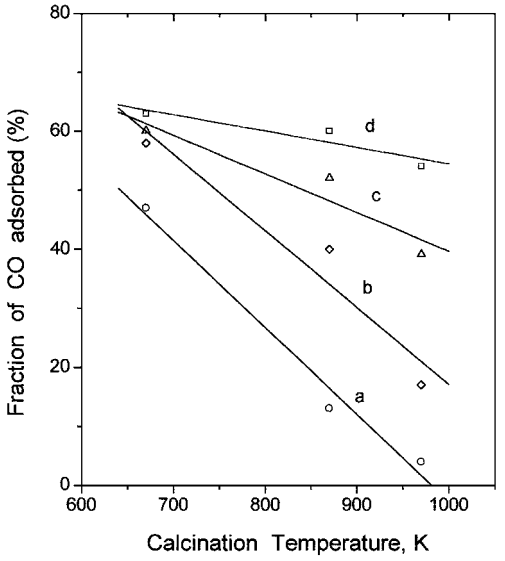

FIG. 8. Effect of calcination on the fraction of CO adsorbed/reacted from a 4.1-μmol pulse of $CO + O_2$ (2 : 1) injected over an Au/Fe_2O_3 catalyst at different temperatures: (a) 300 K, (b) 370 K, (c) 420 K, and (d) 470 K.

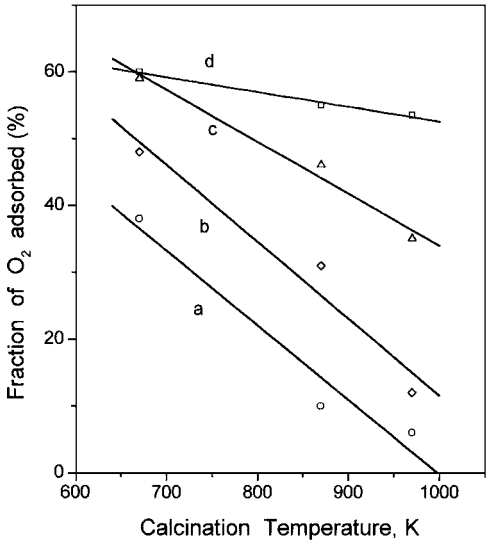

FIG. 9. Effect of calcination on the fraction of O_2 adsorbed/reacted from a 4.1-μmol pulse of $CO + O_2$ (2 : 1) injected over a Au/Fe_2O_3 catalyst at different temperatures: (a) 300 K, (b) 370 K, (c) 420 K, and (d) 470 K.

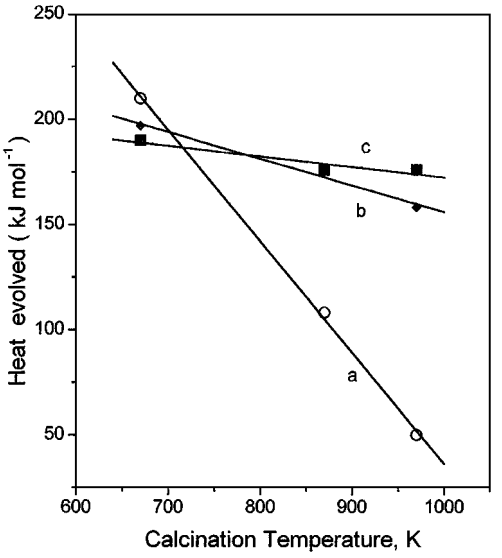

FIG. 11. Effect of calcination on the differential heat evolved during exposure of a Au/Fe_2O_3 catalyst to a 4.1-μmol $CO + O_2$ (2 : 1) pulse at different temperatures: (a) 300 K, (b) 370 K, and (c) 470 K.

conversion was ~95% for a sample calcined at 970 K (Fig. 10a). The corresponding conversions were 75 and 100% at a reaction temperature of 470 K (Fig. 10c).

Figure 11 shows the effect of calcination on the amount of heat produced during $CO + O_2$ (2 : 1) exposure. The calcination of Au/Fe_2O_3 at higher temperatures resulted in a lower q value, the effect being more pronounced at low reaction temperatures (Fig. 11a). At higher reaction temperatures (e.g., 470 K), calcination at temperatures of 670–970 K had a negligible effect; the q value was ~185 kJ mol^{-1} (Fig. 11c).

Calcination Effect on Catalyst Activity

CO oxidation. The Au/Fe_2O_3 catalyst calcined in air at 670 K showed considerable activity at 273 K and a conversion of about 50% was observed in a $CO + O_2 + He$ (2 : 1 : 17) gas flow at 1200 ml h^{-1} g^{-1}. Almost complete conversion was observed at room temperature and above (Fig. 12a). The activity of the catalyst was about the same at calcination up to 770 K but decreased steadily at higher calcination temperatures (Figs. 12b and 12c). Thus, for a catalyst calcined at 970 K, 100% conversion was found at

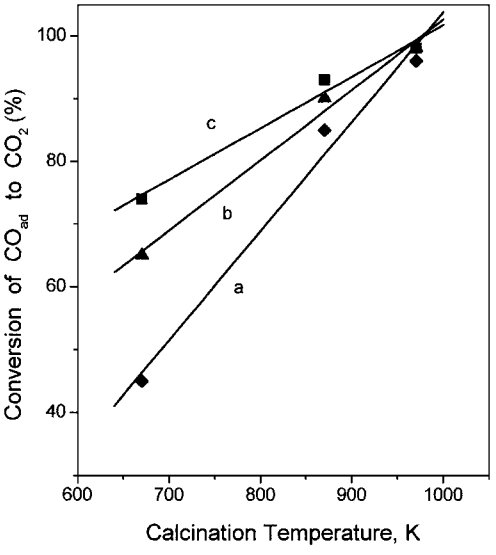

FIG. 10. Effect of calcination on $CO_{ad} \rightarrow CO_2$ conversion when a 4.1-μmol $CO + O_2$ (2 : 1) pulse was injected over a Au/Fe_2O_3 catalyst at different temperatures: (a) 370 K, (b) 420 K, and (c) 470 K.

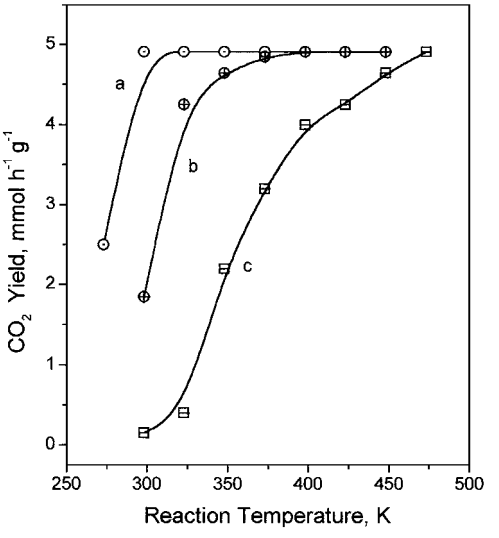

FIG. 12. Effect of calcination on the CO oxidation activity of an Au/Fe_2O_3 catalyst at different reaction temperatures. Measurements with a $CO + O_2 + He$ (2 : 1 : 17) stream at 1.2 L h^{-1} g^{-1} Calcination temperature: (a) 670 K and 770 K, (b) 870 K, and (c) 970 K.

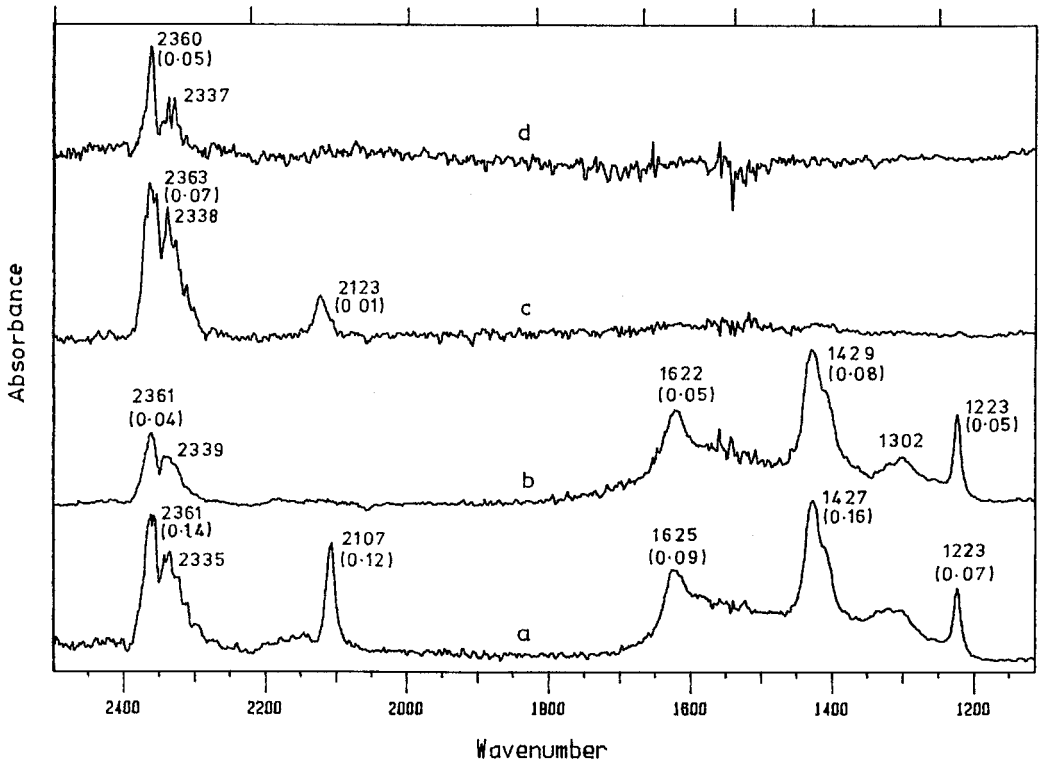

FIG. 13. Infrared band developed on Au/Fe_2O_3 (a) and Fe_2O_3 (b) samples after exposure to 100 Torr CO at 300 K. Spectra c and d are similar for Au/Fe_2O_3 catalysts calcined at 820 and 870 K, respectively, prior to CO exposure. Numbers in parentheses indicate the absorbance values.

~473 K (Fig. 12c), whereas for a catalyst calcined at 670 K, 100% conversion was found only at 298 K (Fig. 12a).

Catalyst bed temperature. At room temperature, the overall temperature of the Au/Fe_2O_3 catalyst rose almost instantly when the catalyst was exposed to a $CO + O_2$ flow; the extent of the increase depended on the temperature at which the catalyst was calcined prior to the flow of $CO + O_2$. Thus, a temperature increase of ~12 K of the catalyst was found for samples calcined at temperatures below 700 K. The corresponding temperature increase was about 10 and 5 K for catalyst samples pretreated at 770 and 870 K, respectively. Furthermore, the overall temperature of the catalyst did not increase when a sample calcined at 970 K was exposed to a $CO + O_2$ flow at 300 K. In addition, an increase in temperature was not detected in experiments performed at higher temperatures or for the $CO + O_2$ reaction over Fe_2O_3 or gold powder at the temperatures used in this study. The increase in temperature, as mentioned above, was stable during an experiment time of 5–6 h.

Infrared Study

Spectra a and b (Fig. 13) show the vibrational bands that developed on the Au/Fe_2O_3 and Fe_2O_3 wafers, respectively, after exposure to 100 Torr CO at ambient temperature. Adsorption of CO on Au/Fe_2O_3 gave rise to a prominent sharp band, ~12-cm^{-1} wide, and with a maximum at around 2107 cm^{-1} (Fig. 13a). No such band was observed on Fe_2O_3 (Fig. 13b). Several overlapping bands at around 1625, 1427, 1406, 1300, and 1223 cm^{-1} due to carbonate-type species are also seen in these spectra in addition to IR bands in the region from 2300 to 2400 cm^{-1} as a result of ν_3 vibrations of CO_2. Coadsorption of CO and O_2 gave rise to a less intense ν(CO) band on Au/Fe_2O_3 and the frequency of this band rose slighly (~2114 cm^{-1}) (18). Similar bands were, however, observed in the other regions of this spectrum for adsorption of $CO + O_2$ on both Au/Fe_2O_3 and Fe_2O_3.

When Au/Fe_2O_3 is calcined at higher temperatures, the intensity of the ν(CO) band and that of the IR bands due to oxygenate species and CO_2 was much lower. Spectra c and d in Fig. 13 show the vibrational bands of the Au/Fe_2O_3 sample calcined at 820 and 870 K and exposed to 100 Torr CO at room temperature. As seen in Fig. 13d, no bands were found in the oxygenate or in the C–O stretching regions at room temperature for adsorption of CO on an Au/Fe_2O_3 sample calcined at 870 K (cf. Fig. 13a).

DISCUSSION

IR Results

A ν(CO) band at ~2107 cm^{-1}, which develops on the Au/Fe_2O_3 but not on the Fe_2O_3 sample (Figs. 13a and 13b), was also reported for the adsorption of CO over Au/ZnO and

Au/TiO_2 (12, 19) and has been assigned to CO molecules bonded at metallic gold sites or at Au/support interfaces (12, 20). Weak bands at higher ν(CO) frequencies, i.e., at $\sim$2160 cm^{-1} (Fig. 13a), may indicate the presence of only a small number of coadsorbed

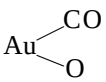

species (11).

As described in detail in (18), the IR bands due to carbonate-like species are found to be thermally stable at temperatures up to 400 K, indicating their limited role in CO_2 formation at low temperatures. Furthermore, the absence of these bands in the calcined samples (Figs. 13c and 13d) where hydroxy group bands were not present suggests the important contribution of OH groups in the formation of carbonate-like species (Figs. 13a and 13b).

In conclusion, the presence of gold facilitates the adsorption of CO at the gold sites or at the gold support interfaces. Carbonate-like species form as a result of the reaction between the hydroxy groups and the CO_2 formed during the interaction of CO or $CO + O_2$ over the catalyst surface. Since the calcined catalyst samples show considerable activity for CO oxidation, even in the absence of carbonate-like species (Figs. 12, 13c, and 13d), and considering the thermal stability of these species at low temperatures, we infer that the carbonate-like species are by-products that do not play an important role in the oxidation of CO over the catalysts used in this study (19).

Microcalorimetry Results

Adsorption and oxidation of CO. A comparison of the data in Figs. 2 and 3 shows that the presence of gold augmented the adsorption/reaction of CO as well as its conversion to CO_2. The role of gold is more pronounced at lower reaction temperatures (<400 K). The q_d value of 125–150 kJ mol^{-1} for the adsorption of CO over Fe_2O_3 (Fig. 3c) is commensurate with the simultaneous occurrence of steps VIII and X (Table 1), i.e., the reaction of CO with lattice oxygen

TABLE 1

Estimated Values of Enthalpy Changes for Reactions Occurring on the Surface of the Au/Fe_2O_3 Catalyst during Exposure to CO, O_2, or $CO + O_2$

Reaction		ΔH (kJ mol^{-1})	Reference
[A] Adsorption step			
$Au + CO \rightarrow Au \cdot CO_{(ad)}$	...I	−42	*a*
		−70	*b*
$2Au + O_2 \rightarrow 2Au \cdot O_{(ad)}$	...II	−145 (at 370 K)	*b*
		−450 (at 420 K)	*c*
$Fe_2O_3 + O_2 \rightarrow Fe_2O_3 \cdot O_{2\,(ad)}$	...III	−130	*d*
$Fe_2O_3 + CO \rightarrow Fe_2O_3 \cdot CO_{(ad)}$	...IV	−105	*e*
[B] Direct reaction of CO and O at gold sites			
$CO_g + \frac{1}{2}O_{2\,ad} \rightarrow CO_2$ (g)	...V	−230	*f*
$CO_{ad} + \frac{1}{2}O_2$ (g) $\rightarrow CO_2$ (g)	...VI	−210	*f*
$CO_{ad} + \frac{1}{2}O_{2\,ad} \rightarrow CO_2$ (g)	...VII	−157	*f*
[C] Redox mechanism involving lattice oxygen of support			
CO (g) $+ 3Fe_2O_3 \rightarrow 2Fe_3O_4 + CO_2$ (g)	...VIII	−50	*g*
$4Fe_3O_4 + O_2 \rightarrow 6Fe_2O_3$	...IX	−460	*g*
[D] Formation of carbonate-like species			
Au/Fe_2O_3 or $Fe_2O_3 + CO_2 \rightarrow$ carbonate bicarbonate and formate species	...X	−80	*h*

[a] Toyoshima, I., and Somorjai, G. A., *Catal. Rev. Sci. Eng.* **19**, 105 (1979), value for polycrystalline gold.
[b] Present study.
[c] Ostrovskii, V. E., and Dobrovolskii, N. N., "Proceedings, 4th International Congress on Catalysis, Moscow, 1968," (B. A. Kazansky, Ed.), Part II, p. 9. Adler, New York, 1968.
[d] Roiter, V. A., Golodets, G. I., and Pyatnitzkii, Yu. I., "Proceedings, 4th International Congress on Catalysis, Moscow, 1968 (B. A. Kazansky, Ed.), Part I, p. 466. Adler, New York, 1968.
[e] Dry, M. E., Shingles, T., Boshoff, L. J., and Oosthuizen, G. J., *J. Catal.* **15**, 190 (1969).
[f] From heat of formation of CO_2 and ΔH value for adsorption steps in [A].
[g] From heat of formation of oxides; "CRC Handbook of Chemistry and Physics" (R. C. Weast, Ed.), CRC Press Inc., Boca Raton, Florida 1980, p. D-71.
[h] Heat evolved during CO_2 adsorption on Au/Fe_2O_3 or Fe_2O_3; present study.

of Fe_2O_3 and subsequent adsorption of product CO_2 to form a carbonate-like species. A slight variation in the q value as a function of temperature can be understood in terms of the relative contribution of these steps at a particular temperature. Similar q values were also found for Au/Fe_2O_3, where a slight difference may be due to the adsorption of a small amount of CO at gold sites (Table 1, step I), which will lead to slightly lower q values (Fig. 2c). The results thus reveal that the reaction with lattice oxygen plays a major role in the interaction of CO with both Au/Fe_2O_3 and Fe_2O_3; the presence of gold augmented this process and will be discussed below.

O_2 adsorption. Similarly, data in Fig. 4 show that the presence of gold augmented the adsorption of O_2, particularly at reaction temperatures below 425 K. The q_d values for the adsorption of O_2 correspond to the enthalpy changes associated with the oxidation of Fe_3O_4 (Table 1, step IX).

$CO + O_2$ adsorption. Figures 5 and 6 show that the presence of gold promoted the adsorption of CO and O_2 to a similar extent when Au/Fe_2O_3 was exposed to a $CO + O_2$ pulse; the overall effect increased with a decreasing sample temperature. The adsorption behavior of both Au/Fe_2O_3 and Fe_2O_3 appears to be the same at 470 K (Figs. 5 and 6), indicating the insignificant role of gold at higher reaction temperatures.

A heat value of $\sim$200 kJ mol^{-1} for the reaction of $CO + O_2$ over both Fe_2O_3 and Au/Fe_2O_3 (Figs. 5 and 6) may be attributed to the simultaneous occurrence of steps VIII–X (Table 1) rather than to a direct reaction of CO and O_2 at gold sites (Table 1, steps V–VII). On one hand, a lower q value ($\sim$125 kJ mol^{-1}) observed in the case of Fe_2O_3 for the reaction of $CO + O_2$ below 400 K (Fig. 6d) indicates a weak adsorption of both CO and O_2. On the other hand, an almost constant q value ($\sim$200 kJ mol^{-1}) for Au/Fe_2O_3 (Fig. 5d) suggests that the presence of gold promoted the adsorption/reaction of both CO and O_2 as well as the conversion of CO to CO_2, particularly below 400 K.

Calcination Effect

Figures 8 and 9 clearly reveal that the calcination of Au/Fe_2O_3 at higher temperatures inhibited the adsorption of both CO and O_2 to a similar extent, the effect being more pronounced at lower adsorption temperatures (Figs. 8 and 9, curves a and b). The q values in Figs. 11b and 11c also suggest the redox mechanism, as mentioned above. At lower reaction temperatures, the q value decreased steadily with an increasing calcination temperature (Fig. 11a), corresponding to the inhibited adsorption of both CO and O_2 and suggesting that steps III and IV (Table 1) play a more important role, giving rise to lower q_d values.

Correlating the above-mentioned data with the TEM (Fig. 1), we infer that the particle size of gold plays an important role in the augmented adsorption and reaction of CO and O_2 over Au/Fe_2O_3, particularly at low reaction temperatures.

Catalyst activity. The steady decrease in the catalytic activity of Au/Fe_2O_3 after calcination at higher temperatures, particularly for CO oxidation at room temperature (Fig. 12c), again reveals the important role of the particle size of gold. Figure 12 also shows that the catalyst activity at a higher reaction temperature (e.g., 470 K) may remain unaffected by the particle size of gold.

Comparing Figs. 5 and 7 reveals that the chemisorption and CO oxidation activity of bulk Au and Au/Fe_2O_3 are quite different. While the ratio $CO(ad)/O_2(ad)$ was above 1 for Au/Fe_2O_3 at reaction temperatures below 450 K, the ratio was always less than 1 for bulk gold under the same conditions. Commensurate with the poor adsorption of both CO and O_2 (Figs. 7a and 7b), bulk gold shows low activity for CO oxidation at temperatures below 400 K (Fig. 7c).

It is, thus, evident that the chemisorption and catalytic properties of Au/Fe_2O_3 for the oxidation of CO at low reaction temperatures are considerably affected by the size of the gold particle. The chemisorption of CO on gold may, in turn, affect the catalytic activity of Au/Fe_2O_3 in the following ways (13):

1. Recombination of chemisorbed CO with oxygen (reaction VI, Table 1) may provide an alternative route.
2. CO chemisorbed at Au sites may spill over to the support, where the activated CO may react at an accelerated rate.
3. Energy released in the chemisorption of CO at Au sites may result in a local surge in temperature at Au/support interfaces, where the Fe_2O_3–CO reaction may occur at an accelerated rate.

On one hand, reaction VI (Table 1) coupled with the adsorption of CO_2 (step X) is expected to result in q values above 250 kJ mol^{-1}, and therefore, the thermochemical data of this study rule out the first possibility. Though these data do not enable us to rule out the possibility of spillover, a number of questions arise concerning the validity of this mechanism (21): What is the energy requirement for the activated atom/molecule to jump across the interface? What is the likelihood of a molecule retaining its activation during transfer from the metal to the support? What is the likelihood of simultaneous spillover of more than one of the reactants? What is the nature of the molecular excitation? All these questions are, as yet, unanswered. On the other hand, the rise in temperature at the metal/support interfaces (13) was also found in this study.

We thus reached the following conclusions: The oxidation of CO on both Fe_2O_3 and Au/Fe_2O_3 occurs via a similar reaction mechanism; i.e., it involves reduction and

reoxidation of the Fe_2O_3 bulk (22). In the case of Au/Fe_2O_3, the energy released due to the chemisorption of CO at metal sites may result in an increase in temperature at the metal support interfaces, where the Fe_2O_3–CO reaction may occur at an accelerated rate. The observed rise in the temperature of the catalyst bed during flow of a $CO + O_2$ gas stream over Au/Fe_2O_3 at room temperature, when the promotional effect of gold is more pronounced (Figs. 2–6 and 12), is in agreement with this conclusion.

Even though the increase in the equilibrium temperature was only slight (~10–15 K), the actual temperature surge at the metal support interfaces may be much higher. The extent of this increase probably depends on the size of the gold particles, since the heat produced during chemisorption (Δq) = mass of crystallite (m) × specific heat of Au (s) × temperature increase (ΔT). ΔT will thus depend on the size of the crystallite; the smaller crystallites will show a greater increase in temperature. The increase in temperature at the metal support interface may, however, also depend on other factors such as the nature of the metal contact and the conductivity of the support. The decreasing promotional effect of gold in the calcined samples (Figs. 8–12), when the gold particles may acquire bulk properties and the ΔT may be negligible, agrees with our hypothesis. The multiple surface temperature studies by Kaul and Wolf (23) show the existence of localized hot spots in the regions where the rate of CO oxidation on Pt/SiO_2 and Pd/SiO_2 is higher. The existence of CO islands, with highly reactive boundaries, during CO oxidation on Pt/SiO_2 and Pd/SiO_2 has also been proposed by Gonzalez *et al.* (24).

Several research groups (1, 2) recognized the importance of the nanosize Au particles for the high catalytic activity of supported gold catalysts. It has been suggested that the small gold particles have different surface properties compared to bulk Au and some kind of electronic interaction of the metal and the support is thought to be responsible for this difference (19). We saw no shift in the Au_{4f} binding energy and no oxidized Au was observed in our XPS study on Au/Fe_2O_3. The formation of Au^{1+} during the adsorption of CO or $CO + O_2$ (20) occurs to a very limited extent, if at all (Fig. 13). This agrees with recent XPS and ISS studies conducted by Epling *et al.* (25), which show the presence only of Au^0 on the surface of an Au/Fe_2O_3 catalyst. We therefore conclude that the effect of the particle size of gold may be due to the effects of geometry, as discussed by Che and Bennett (26), rather than to modified electronic properties. Recent surface science studies have demonstrated that the concentration of crystallographic defects, associated with the surface of metal single crystals, has considerable influence on their adsorption and catalytic properties and that these concepts may be applicable to the small metal particles with atoms of lower coordination than the bulk (27).

SUMMARY

Our results contradict the conclusions drawn in some of the recent studies:

1. We did not find more than one kind of gold metal site in Au/Fe_2O_3, before and after CO adsorption, in contrast to Boccuzzi *et al.* (11, 12, 20).
2. Thermochemical data of this study suggest that there are not two pathways for CO oxidation on Au/Fe_2O_3 and Fe_2O_3, as proposed earlier (20).
3. Carbonate-like species may not play a significant role in CO oxidation, as suggested in Ref. (7).

We conclude that CO oxidation occurs via a similar redox mechanism on both Fe_2O_3 and Au/Fe_2O_3 catalysts. The promotional effect of gold in augmented CO oxidation activity is attributed to the CO chemisorption at small (nanosize) gold particles. It is proposed that the energy released during the chemisorption of CO leads to a local surge in temperature at Au/Fe_2O_3 interfaces, while the temperature of the catalyst bulk may be affected only slightly. Such metal support interfaces may, thus, be the sites at which an accelerated Fe_2O_3–CO reaction and subsequent reoxidation of the support occurs, particularly at low reaction temperatures when the temperature of the catalyst is not high enough to overcome the energy barrier. In other words, the chemisorption of CO at Au sites supplies some of the energy required for the above-mentioned reactions, energy which would otherwise be available only by increasing the temperature of the system. As discussed above, such phenomena will occur only in the case of very small metal particles.

ACKNOWLEDGMENTS

We thank the Editor, Professor Roel Prins, for going through the manuscript critically and for his valued suggestions for the improvement of the manuscript.

REFERENCES

1. Haruta, M., Yamada, N., Kobayashi, T., and Iijima, S., *J. Catal.* **115**, 301 (1989).
2. Haruta, M., Tsubota, S., Kobayashi, T., Kageyama, H., Genet, M. J., and Delmon, B., *J. Catal.* **144**, 175 (1993).
3. Bollinger, M. A., and Vannice, M. A., *Appl. Catal. B* **8**, 417 (1996).
4. Knell, A., Barnickel, P., Baiker, A., and Wokaun, A., *J. Catal.* **137**, 306 (1992).
5. Gardner, S. D., Hoflund, G. B., Upchurch, B. T., Schryer, D. R., Kielin, E. J., and Schryer, J., *J. Catal.* **129**, 114 (1991).
6. Hoflund, G. B., Gardner, S. D., Schryer, D. R., Upchurch, B. T., and Kielin, E. J., *Appl. Catal. B* **6**, 117 (1995).
7. Boccuzzi, F., Chiorino, A., Tsubota, S., and Haruta, M., *Catal. Lett.* **29**, 225 (1994).
8. Tanielyan, S. K., and Augustine, R. L., *Appl. Catal. A* **85**, 73 (1992).
9. Visco, A. M., Donato, A., Milone, C., and Galvagno, S., *React. Kinet. Catal. Lett.* **61**, 219 (1997).

10. Salama, T. M., Shido, T., Minagawa , H., and Ichikawa, M., *J. Catal.* **152**, 322 (1995).
11. Minico, S., Scire, S., Crisafulli, C., Visco, A. M., and Galvagno, S., *Catal. Lett.* **47**, 273 (1997).
12. Boccuzzi, F., Chiorino, A., Tsubota, S., and Haruta, M., *J. Phys. Chem.* **100**, 3625 (1996).
13. Gangal, N. D., Gupta, N. M., and Iyer, R. M., *J. Catal.* **126**, 13 (1990).
14. Gangal, N. D., Gupta, N. M., and Iyer, R. M., *J. Catal.* **140**, 443 (1993).
15. Tripathi, A. K., and Gupta, N. M., *J. Catal.* **153**, 208 (1995).
16. Tripathi, A. K., Gupta, N. M., Chatterji, U. K., and Iyer, R. M., *Ind. J. Technol.* **30**, 107 (1992).
17. Gupta, N. M., Kamble, V. S., Iyer, R. M., Thampi, K. R., and Gratzel, M., *J. Catal.* **137**, 473 (1992).
18. Tripathi, A. K., Kamble, V. S., and Gupta, N. M., to be published.
19. Lin, S. D., Bollinger, M., and Vannice, M. A., *Catal. Lett.* **17**, 245 (1993).
20. Boccuzzi, F., and Chiorino, A., *J. Phys. Chem.* **100**, 3617 (1996).
21. Bond, G. C., Fuller, M. J., and Molloy, L. R., *in* "Proceedings, 6th International Congress on Catalysis, London, 1976" (G. C. Bond, P. B. Wells, and F. C. Tompkins, Eds.), Vol. I, p. 356. The Chemical Society, London, 1977.
22. Sakata, K., Veda, F., Misono, M., and Yoneda, Y., *Bull. Chem. Soc. Jpn.* **53**, 324 (1980).
23. Kaul, D. J., and Wolf, E. E., *J. Catal.* **91**, 216 (1985); *J. Catal.* **93**, 321 (1985).
24. Dirk Boecker, Y. L., and Gonzalez, R. D., *J. Catal.* **110**, 319 (1988).
25. Epling, W. S., Hoflund, G. B., Weaver, J. F., Tsubota, S., and Haruta, M., *J. Phys. Chem.* **100**, 9929 (1996).
26. Che, M., and Bennett, C. O., in "Advances *in* Catalysis" (D. D. Eley, H. Pines, and P. B. Weisz, Eds.), Vol. 36, p. 76. Academic Press, San Diego, CA, 1989.
27. Somorjai, G. A., *in* "Advances in Catalysis" (D. D. Eley, H. Pines, and P. B. Weisz, Eds.), Vol. 26, p. 1. Academic Press, San Diego, CA, 1977.